# Development of a night-time radiative sky cooling production & storage system: A proposal for a robust sizing and potential estimation methodology

Zakaria Aketouane, Denis Bruneau, Alain Sempey, Ryad Bouzouidja, Philippe Lagiere, Saed Raji, Pierre Roger

▶ **To cite this version:**

Zakaria Aketouane, Denis Bruneau, Alain Sempey, Ryad Bouzouidja, Philippe Lagiere, et al.. Development of a night-time radiative sky cooling production & storage system: A proposal for a robust sizing and potential estimation methodology. Applied Thermal Engineering, 2022, 211, pp.118378. 10.1016/j.applthermaleng.2022.118378 . hal-03782126

**HAL Id: hal-03782126**
**https://hal.science/hal-03782126**

Submitted on 22 Jul 2024

**HAL** is a multi-disciplinary open access archive for the deposit and dissemination of scientific research documents, whether they are published or not. The documents may come from teaching and research institutions in France or abroad, or from public or private research centers.

L'archive ouverte pluridisciplinaire **HAL**, est destinée au dépôt et à la diffusion de documents scientifiques de niveau recherche, publiés ou non, émanant des établissements d'enseignement et de recherche français ou étrangers, des laboratoires publics ou privés.

Distributed under a Creative Commons Attribution - NonCommercial 4.0 International License

Version of Record: https://www.sciencedirect.com/science/article/pii/S1359431122003350
Manuscript_6f08d84c950576e23e26ffd15f86a518

# Development of a night-time radiative sky cooling production & storage system: a proposal for a robust sizing and potential estimation methodology

Zakaria AKETOUANE[1,2,3], Denis BRUNEAU[2], Alain SEMPEY[1*], Ryad BOUZOUIDJA[1], Philippe LAGIERE[1], Saed RAJI[3], Pierre ROGER[3]

[1] Université de Bordeaux, UMR CNRS 5295, I2M Bordeaux, 351 cours de la Libération, F-33400 Talence, France

[2] Ecole Nationale Supérieure d'Architecture et de Paysage de Bordeaux, Laboratoire GRECCAU, 740 cours de la Libération, CS 70109, 33405 Talence cedex, France

[3] Nobatek/INEF4, 64600 Anglet, France

***corresponding author: alain.sempey@u-bordeaux.fr**

## Abstract

This paper proposes a sizing method to guide the design of water-circulating radiative sky cooling systems and water-based energy storage solutions. Following this method, the choice of operational flow rate in the radiative sky cooling (RSC) panels and the water storage is based on four indicators: sub-ambient temperature, cooling power density, minimum storage temperature and useful energy stored. The method is applied to the BaityKool Solar Decathlon Middle East (SDME) prototype in order to design a water-radiative sky cooling system with storage in the climatic conditions of Dubai. We developed passive strategies for the BaityKool prototype, including a multi-functional innovative exterior wall and a semi-indoor courtyard space, combined with active solutions (in particular a hydraulic radiative sky cooling system). The experimental campaign conducted on the RSC system over three successive nights in November (ambient air temperature between 22.7 to 31.4°C) indicates an average cooling power of 30-45 W $m^{-2}$ for a maximum sub-ambient temperature drop of



© 2022 published by Elsevier. This manuscript is made available under the CC BY NC user license
https://creativecommons.org/licenses/by-nc/4.0/

25 2.8°C, and shows that great attention to the water pipes and storage insulation can lead to an
26 increase in the thermal performance of radiative sky cooling systems.

27 **Keywords:** Radiative sky cooling; design method; thermal modeling; extreme climate
28 conditions; effective sky temperature; energy balance model

**Nomenclature**

| | |
|---|---|
| a | Coefficient (-) |
| A | External surface of the storage tank ($m^2$) |
| $A_{rsc}$ | Area of the RSC panels ($m^2$) |
| $A_p$ | External surface of the pipe ($m^2$) |
| b | Coefficient (-) |
| $Cp_s$ | Heat capacity of the fluid in the storage tank ($J\ kg^{-1}K^{-1}$) |
| $Cp_w$ | Water heat capacity ($J\ kg^{-1}K^{-1}$) |
| $e_{aal}$ | Thickness of the anodized Aluminum (m) |
| $e_{al}$ | Thickness of the Aluminum (m) |
| $e_g$ | Thickness of the glue (m) |
| $e_{is}$ | Thickness of the insulation (m) |
| $e_p$ | Thickness of the panel (m) |
| $E_{useful}$ | Useful energy in the storage system (J) |
| $e_{wi}$ | Depth of the water (m) |
| F' | Collector efficiency (-) |
| $h_{cv}$ | External convective exchange coefficient ($W\ m^{-2}\ K^{-1}$) |
| $h_f$ | Internal convective heat transfer coefficient between the fluid and the walls of the channel ($W\ m^{-2}\ K^{-1}$) |
| $h_p$ | Overall heat exchange coefficient along the pipe ($W\ m^{-2}\ K^{-1}$) |
| $h_{rs}$ | Radiation heat exchange coefficient between the surface of the panel and the sky ($W\ m^{-2}\ K^{-1}$) |
| $I_s$ | Short wavelength solar radiation ($W\ m^{-2}$) |
| $k_{is}$ | Thermal conductivity of the insulation ($W\ m^{-1}\ K^{-1}$) |

$k_w$ Water thermal conductivity (W $m^{-1}$ $K^{-1}$)

L Length (m)

$L_g$ Length of the glue (m)

$L_p$ Length of the panel (m)

$l_p$ Width of the panel (m)

$L_{wi}$ Length of the heat transfer fluid channel (m)

$\dot{m}$ Flow rate through the hydraulic circuit (kg $s^{-1}$)

$m_s$ Mass of the fluid (kg)

n Coefficient (-)

Nu Nusselt number (-)

$P_{c,l}$ Output power of the cooling load (W)

$P_{elec}$ Electrical power consumed by the pump (W)

$P_{l,p}$ Thermal loss to the ambient air (W)

$P_{l,s}$ Thermal loss from the tank (W)

$P_p$ Perimeter of the panel (m)

Pr Prandtl number (-)

$P_{RSC}$ Power of RSC (W)

$P_{th\text{-}diss}$ Thermal loss from the pump (W)

r Channel form factor (-)

R Solar heat flux density absorbed by the panel in the infrared spectrum (W $m^{-2}$)

Re Reynolds number (-)

S Solar heat flux density absorbed by the panel in the visible spectrum (W $m^{-2}$)

$T_a$ Temperature of ambient air (K)

$\hat{T}_a$ Average ambient temperature (K)

$T_{al}$ Front surface temperature of the panel (K)

$T_{fi}$ Temperature of inlet water (K)

$T_{fo}$ Temperature of outlet water (K)

$T_s$ Average storage temperature of the tank (K)

$T_{s,exp,i}$ Measured water storage temperature (K)

$T_{s,min}$ Minimum storage temperature in the early morning (K)

$T_{s,num,i}$ Modeled water storage temperature (K)

$T_{set}$ Desired set temperature in the cooled room (K)

$T_{sky}$ Average value of effective sky temperature (K)

U Heat loss coefficient (W $m^{-2}$ $K^{-1}$)

UA Overall heat exchange coefficient of the storage tank (W $K^{-1}$)

$U_L$ Overall heat loss coefficient of the panel (W $m^{-2}$ $K^{-1}$)

$U_t$ Top heat loss coefficient of the panel (W $m^{-2}$ $K^{-1}$)

$U_b$ Bottom heat loss coefficient of the panel (W $m^{-2}$ $K^{-1}$)

$U_e$ Edge heat loss coefficient of the panel (W $m^{-2}$ $K^{-1}$)

$V_s$ Storage volume of the tank ($m^3$)

$\hat{V}_w$ Average wind speed (m $s^{-1}$)

$V_w$ Wind speed (m/s)

α Solar absorption coefficient of the external surface of the panel (-)

$\Delta T_{sub-a}$ Sub-ambient temperature drop (K)

ε Emissivity (-)

η Pump efficiency (-)

λ Thermal conductivity of the fluid (W $m^{-1}$ $K^{-1}$)

μ Dynamic viscosity of the fluid (Pa $s^{-1}$)

ρ Density (kg $m^{-3}$)

σ Boltzmann coefficient (W $m^{-2}$ $K^{-4}$)

**Abbreviations**

| | |
|---|---|
| BIPV | Building-Integrated Photovoltaic |
| HVAC | Heating, ventilation, and air conditioning |
| NSC | Night Sky Cooling |
| PVT | Photovoltaic thermal |
| RMSE | Root mean square error |

| | |
|---|---|
| RSC | Radiative Sky Cooling |
| SDME | Solar Decathlon Middle East |
| TEC | Thermoelectric cooler |

## 1 Introduction

The world today is experiencing significant growth and urbanization, both synonymous with high energy consumption. The building sector accounts for about 42% of world energy consumption due to the intensive use of heating, ventilation, and air conditioning (HVAC) systems for heating and cooling combined with the low performance of building envelopes [1]. The use of efficient systems for cooling is a major issue to reduce energy bills as well as greenhouse gas emissions.

Radiative Sky Cooling (RSC), or Night Sky Cooling (NSC), is a promising passive solution to dissipate heat with low energy consumption. The principle is to exploit the sky as a radiative heat sink where the temperature is colder than in our immediate environment; this can be achieved by exchanging heat by longwave radiation between 8-14 μm where the atmosphere is transparent (atmospheric window). This phenomenon depends largely on location and climatic conditions, such as wind speed, sky cover and humidity [2–5].

Many researchers have investigated different approaches to exploit night-time RSC on building roofs by means of air and water systems. The average cooling power using these techniques ranges between 30-50 W $m^{-2}$ [6]. Liu et al. [7] designed a duct-type heat exchanger installed on the roof of a building in Hohhot (China) to produce cool air during summer nights and reduce solar absorption during the day. An air system of this kind can reduce the inlet air temperature by 6.8°C in a cold semi-arid (steppe) climate [8]. Meir et al. [9] used an unglazed polymer flat plate radiator with water circulation as an economical alternative to active systems on a building located in Oslo, Norway. Their 5.3 $m^2$ radiative sky panel was coupled to a storage tank to evaluate cold production during the night. It was shown that in a warm

summer humid continental climate, such a panel can cool down a 280 L storage tank by 20°C. Other experiments have been carried out in different locations and weather conditions around the world. Al-Nimr et al. [10] showed that a water circulation RSC panel in Irbid, Jordan (Mediterranean Climate) with an area of 0.6 m² can cool down a 120 L storage tank by 15°C. A roof constructed with embedded water pipes was installed in Greece (Mediterranean Climate) by Dimoudi and Androutsopoulos [11] showing a radiative cooling power ranging from 9.5 W $m^{-2}$ to 97.8 W $m^{-2}$. Tevar et al. [12] tested three RSC panels in Almeria, Spain (hot semi-arid-steppe climate) with high, medium and low emittance; maximum cooling power (63.7 W $m^{-2}$) was naturally observed for the organic panel with high emissivity while the panel with medium emittance resulted in 42.2 W $m^{-2}$ and the one with low emissivity in 7.7 W $m^{-2}$. In Owerri, Nigeria (Tropical monsoon climate), Okoronkwo et al. [13] conducted an experimental study using a RSC panel made of steel pipes and covered by an aluminum sheet to cool a water storage tank during the night; the cooled water was used during the day to maintain a room temperature between 26°C and 28°C by circulating it through a heat exchanger for space cooling. Bokor et al. [14] evaluated experimentally a commercial transpired solar air collector for night-time cold production by RSC. The maximum cooling performance measured was 66.5 $Wm^2$ for an average value of 34.6 W $m^{-2}$ in Erding, Turkey. A combination of uncovered photovoltaic thermal (PVT) panels and RSC was investigated by Eicker and Dalibard [15] to provide electricity during the day and cooling energy during the night; the cooling power measured depends on the use of the cold production, and was estimated at between 60-65 W $m^{-2}$ for cooling a warm water storage tank and 40-45 W $m^{-2}$ for cooling a ceiling. Chen et al. [3] compared glazed/unglazed PVT with switchable film insulation in a Tropical climate (Sanya, China). They found that PVT panels with film insulation satisfactorily combine solar thermal cooling and nocturnal passive cooling performances, with an annual total energy yield that is 10% and 32% higher than that of glazed and unglazed PVT collectors. The same combination was used by Zhao et al. [16]

using air as a heat carrier to produce cool air for buildings during the night. To enhance the space cooling energy density, Kwan et al. [17] investigated coupling PV panels and thermoelectric cooler (TEC) modules in two functioning modes (with and without batteries). Aketouane et al. [18] simulated energy-saving potential by coupling a watertowater heat pump and a water-cooling RSC system; this reduces the electrical consumption of the heat pump by up to 20% over the summer period. Recently, in order to enhance radiative sky cooling production over 24h, some authors have also achieved radiative cooling during the day using surfaces that combine high solar reflection and high thermal emission; these surfaces were produced from high-technology materials such as ultrabroadband photonic structures or scalable-manufactured glass-polymer hybrid metamaterials [19–28]. For example, Goldstein et al. [29] built a circulated water-cooling system (total panel surface area of 0.74 $m^2$), with a surface of a visibly-reflective extruded copolymer mirror on top of an enhanced silver reflective surface [30], and showed a temperature drop of between 3°C and 5°C under a flow rate of 12 L $h^{-1}$ $m^{-2}$. Similarly, Zhao et al. [31] studied a kilowatt-scale radiative cooled-cold collection system with 13.5 $m^2$ radiative cooling surface area, and investigated the influence of two flow rate strategies: controlling intermittent flow and continuous flow to produce water with constant sub-ambient temperatures, and maximizing cooling energy generation; their RSC system provided a maximum cooling power of 1296 W at night at a water volumetric flow rate of 26.5 L $h^{-1}$ $m^{-2}$).

Most of the RSC systems cited previously produce cold air or water during the night-time, or during night-time and daytime, using high-technology film composites or metamaterials to enhance the response to achieve higher cooling needs. Another common point in these studies is the evaluation of cooling production based solely on climatic conditions, whereas system performances depend on the cooling needs (especially the temperature of the fluid to be cooled), the size and the design of the RSC installation. These

new coatings are capable of radiative cooling during daytime and even under intense solar radiation, and will have a major impact on the energy consumption of buildings if combined with passive [4,32,33] or active techniques [18,29,34]. Since the latest promising advances in Daytime Radiative Sky Cooling, various strategies have been explored to improve the thermal performance of this technology [35]. Nevertheless, for commercial and technological diffusion reasons, in this paper we choose to work on the dimensioning and experimentation of a low-technology night-time RSC production-storage-distribution system, using panels made of a classic commercial material, anodized steel.

Using numerical modeling and experimental calibration, the aim of this article is firstly to propose a sizing method, which simultaneously guides the choice of the operating flow in the RSC panels and the choice of the water storage volume. Previous studies [e.g. [29,36]] based the RSC panel model only on the flow rate. We propose to go further and also size the tank volume so that the whole system performs to respond to cooling needs, even depending partially on the roof surface available to house RSC panels. Secondly, we evaluate performance of the whole system (and improvement potential) under extreme weather and sand storm conditions (near Dubai city). The aim of this paper is to guide the design of RSC systems in order to meet the cooling demand.

The remainder of this study is organized as follows. Section 2 describes the RSC panels. Section 3 investigates the RSC sizing method. Sections 4 and 5 present the study areas, data, and methods. Section 6 discusses the performance of the RSC panels and section 7 concludes this study.

# 2 Description and modeling of the RSC System

## 2.1 Presentation of the RSC system

In the Solar Decathlon Middle East (SDME) Dubai 2018 [37], a water-circulating RSC system was developed for the BaityKool project [38].

In this study, the BATISOL® unglazed solar collector is considered. It was first developed and tested by Nobatek-INEF4 as an Innovative Thermal Solar Façade [39], and is used in this study, on the roof of BaityKool, as an RSC panel to produce cooled water during the night. This panel consists of an anodized aluminum front plate measuring 600 mm × 1200 mm × 2 mm and an aluminum rear plate of the same dimensions (see Figure 1a). The two plates are assembled with glue deposited to form circuits in which the heat transfer fluid (water in our case) circulates in the panel. The whole is insulated with 40 mm of expanded polystyrene and assembled with two panels in each metal frame, as presented in Figure 1b.

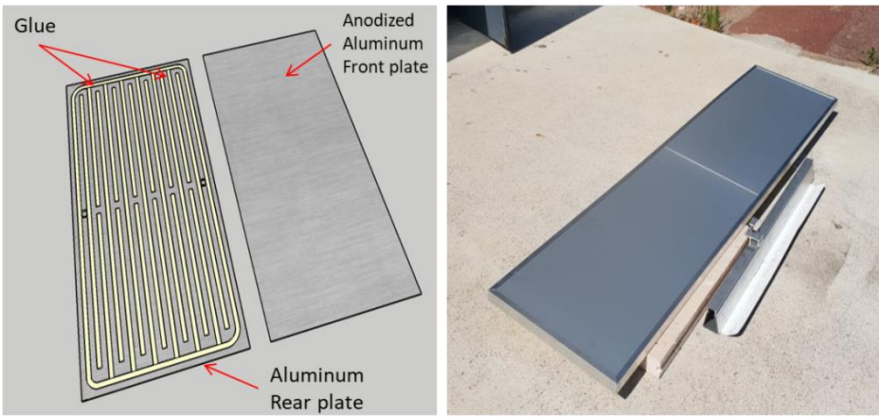


**Figure 1 (a) Diagram of BATISOL® RSC panel composition, (b) Photo of two RSC panels insulated and assembled on the same metal frame.**

Anodized aluminum has been chosen here as the front plate of the RSC panel, because it has excellent radiative properties in the infrared radiation range between 8-14 µm, corresponding to the atmospheric window. Using an EM4 Emissometer from Themacs

Engineering [40], the normal emissivity of this anodized aluminum has been estimated to be 0.96.

The proposed RSC system is presented in Figure 2. It consists of RSC panels that cool down a storage tank during the night. The stored cold water is then used for cooling one of the rooms in the BaityKool house (cold diffusion) during the day using radiative panels.

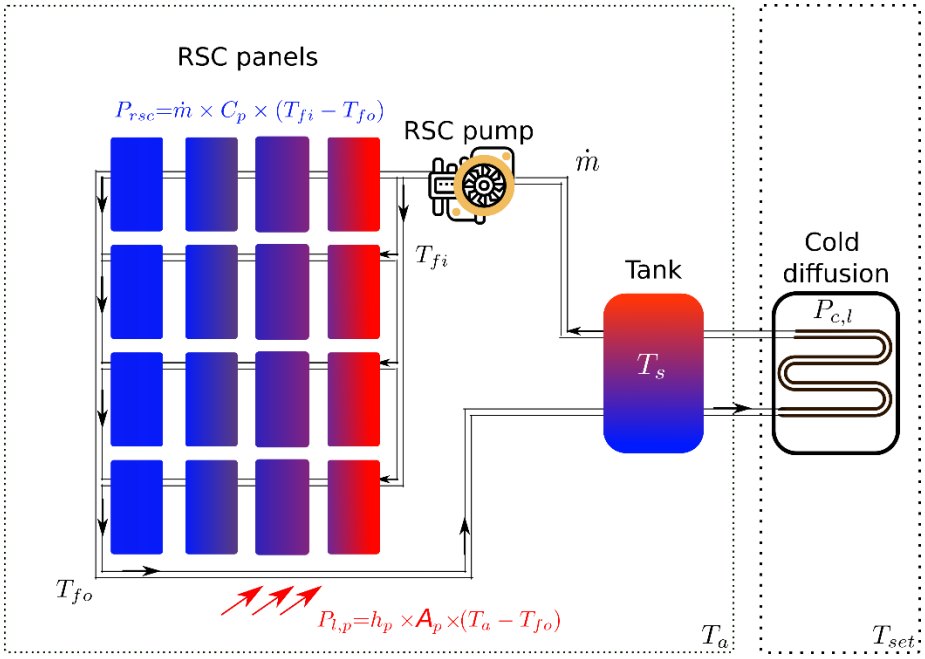


**Figure 2 Schematic representation of the Radiative Sky Cooling (RSC) system developed and installed in the BaityKool house. $P_{l,p}$ is the heat loss (heat gains) from the pipe to the ambient air. $h_p$ is the heat exchange coefficient by convection between the pipes and the ambient air (W m$^{-2}$ K$^{-1}$). $P_{c,l}$ is the cooling load of the considered room in BaityKool. $P_{RSC}$ is the RSC power produced by the panel.**

## 2.2 Modeling the RSC system

### 2.2.1 RSC panel model

The following thermal modeling is considered to describe the RSC panel behavior. This model is based on the well-known Duffie and Beckmann equation for a flat plate solar collector [41], used by Farmahini Farahani et al. [4]. It represents the outlet water temperature $T_{fo}$ (K) (Eq. 10) of the RSC panels as a function of the inlet water temperature $T_{fi}$ (K):

$$\frac{T_{fo} - T_a - (S-R)/U_L}{T_{fi} - T_a - (S-R)/U_L} = exp\left(-\frac{U_L A_{rsc} F'}{\dot{m} C_p}\right) \quad \text{Eq. 1}$$

158 $A_{rsc}$ ($m^2$) is the area of the panel. $\dot{m}$ (kg $s^{-1}$) represents the flow rate through the hydraulic
159 circuit. $F'$ (-) is the collector efficiency factor. $U_L$ (W $m^{-2}$ $K^{-1}$) is the overall heat loss
160 coefficient. In addition to the solar heat flux density absorbed by the panel $S$, the term $R$ has
161 been added to the equation to consider the net radiative flux density exchanged in the far
162 wavelength in the infrared radiation between the panel surface (at temperature $T_{al}$) and the
163 sky. A detailed description of the model can be found in Appendix A.

164 **2.2.2 Storage tank model**

165 The thermal behavior of the storage tank can be predicted using the following energy
166 balance, based on studies by Aili et al. [36] and Goldstein et al. [29]. Five forms of heat flow
167 are taken into account, namely $P_{RSC}$ cooling power, $P_{l,p}$ heat gain from the pipes, $P_{l,s}$ heat gain
168 from the storage tank, $P_{c,l}$ cooling load and $P_{th,pump}$ heat gain from the pump:

$$m_s Cp_s \frac{dT_s}{dt} = P_{RSC} - P_{l,p} - P_{l,s} - P_{c,l} - P_{th-pump} \quad \text{Eq. 2}$$

169 where $m_s$ is the fluid mass (kg). $T_s$ is the average storage temperature of the tank (K). $Cp_s$ is
170 the heat capacity of the fluid (J $kg^{-1}$ $K^{-1}$). $P_{RSC}$ is the cooling power (W) generated by the
171 RSC panels:

$$P_{RSC} = \dot{m} \times C_p \times (T_{fo} - T_s) \quad \text{Eq. 3}$$

172 Unfortunately, part of this cooling power is not effective: there may be some heat gains $P_{l,p}$
173 from the ambient air along the pipe that links the RSC panels to the storage tank:

$$P_{l,p} = h_p \times A_p \times (T_{fo} - T_a) \quad \text{Eq. 4}$$

where $h_p$ is an overall exchange coefficient along these pipes (W m$^{-2}$ K$^{-1}$), $A_p$ is the area of pipes (m$^2$), and $T_a$ is the ambient air temperature (K). Thermal losses (heat gains) $P_{l,s}$ (W) from the tank to the ambient air are expressed as follows:

$$P_{l,s} = U \times A \times (T_s - T_a) \quad \text{Eq. 5}$$

where $U{\cdot}A$ is the overall heat exchange coefficient (W K$^{-1}$) between the storage tank and the ambient air. $P_{c,l}$ is the cooling load (W) of the considered room (cf. Figure 2).

$$P_{th-diss} = (1 - \eta) \times P_{elec} \quad \text{Eq. 6}$$

where $\eta$ is the pump efficiency (-) and is equal to 0.8. $P_{elec}$ is the electrical power consumed by the pump (W).

## 3 Sizing Method

In a given building, every effort is made to fulfil the cooling requirements using RSC. The production per m² of such systems for fluid temperature around an ambient air temperature range is about 50 W m$^{-2}$ [6]; thus, it is often the available surface area on the roof that sizes the surface of RSC panels $A_{RSC}$, and not the cooling needs of the building, which are often greater. Hence our choice of a sizing method that considers a fixed value for $A_{RSC}$. Here we propose a robust method which allows the choice of flow rate $\dot{m}$ based on the methodology of Aili et al. [36] and Goldstein et al. [29] and the water storage volume $V_s$ based on the following 4 indicators:

- sub-ambient temperature drop $\Delta T_{sub\text{-}a} = T_a - T_{fo}$ (K) [29,36,42]
- cooling power density $P_{RSC}/A_{RSC}$ *(W m$^{-2}$)* [29,36,42]
- minimum storage temperature in the early morning (after night cooling period) $T_{s,min}$ *(K)*
- useful energy (stored in the storage system) $E_{useful}$ *(J)*

We improve the design of an RSC panel by adding two indicators, namely $T_{s,min}$ and $E_{useful}$. In fact, the RSC system works mainly during the night to cool the tank to a minimum temperature value. During the daytime, the need for cooling in the house involves using the stored cold water, which contributes to the increase in the storage temperature (in the BaityKool prototype, this stored cold water circulates in panels that constitute the kitchen credenza). The storage system must therefore both assume the amount of energy required for cooling and ensure a lower cooling water temperature than the desired set temperature in the cooled room $T_{set}$. The useful energy present in the storage tank is then calculated as:

$$E_{useful} = m_s \times Cp_s \times (T_{set} - T_{s,min}) \quad \text{Eq. 7}$$

In this work, we assume a set temperature value around $T_{set}$ = 26°C [43]. The proposed method is based on the four indicators defined above and is carried out in two stages (see Figure 3):

- 1st step: Choice of flow rate of water $\dot{m}$ in the RSC panels *(considering only the behavior of the panel, without storage)*

  In this step, 0 is used to calculate $P_{RSC}$ and $\Delta T_{sub\text{-}a}$ depending on the flow rate per unit area $\dot{m}/A_{RSC}$ (l min-1 $m^{-2}$). The average values of $\bar{T}_a$, $\bar{T}_{sky}$ and $\bar{V}_w$ during a typical night are needed as input for the model. In order to calculate the temperature drop $\Delta T_{sub\text{-}a}$, we assume that the water inlet temperature is equal to the ambient temperature $(T_{fi}=T_a)$ [29]. Therefore, Eq. 1 becomes:

  $$\frac{T_{fo} - T_a - (S-R)/U_L}{(S-R)/U_L} = exp(-\frac{U_L A_{rsc}\, F'}{\dot{m}\, C_p}) \quad \text{Eq. 8}$$

  Based on the calculation results, the flow rate should be chosen either to maximize $P_{RSC}$ or depending on the application needed.

- 2nd step: Choice of storage volume $V_s$ *(considering entire system with storage)*

After choosing the flow rate and fixing the total area $A_{RSC}$ of the RSC panels, $\boldsymbol{T_{s,min}}$ is determined by the overall energy balance of the system (see Eq. 9) that combines Eq. **1**; Eq. **2** and considers ($T_{fi}$=$T_s$):

$$m_s Cp_s \frac{dT_s}{dt} = \dot{m}\, C_p\, (T_{fo} - T_s) - P_{l,p} - P_{l,s} - P_{c,l} - P_{th-pump} \qquad \text{Eq. 9}$$

$$\text{Where } T_{fo} = \left(T_{fi} - T_a - \frac{S-R}{U_L}\right) \times exp\left(-\frac{U_L A_{rsc}\, F'}{\dot{m}\, C_p}\right) + \left(T_a - \frac{S-R}{U_L}\right) \qquad \text{Eq. 10}$$

$\boldsymbol{E_{useful}}$ is calculated using Eq. **7**. Hourly values of $I_s$, $T_a$, $T_{sky}$, $V_w$ and $P_{c,l}$ during two typical days are needed as input for the model. The storage system is then sized based on the results of $T_{s,min}$ and $E_{useful}$ depending on the storage volume. The chosen volume must be sufficient to cover the total or partial energy needs for cooling the room under consideration.

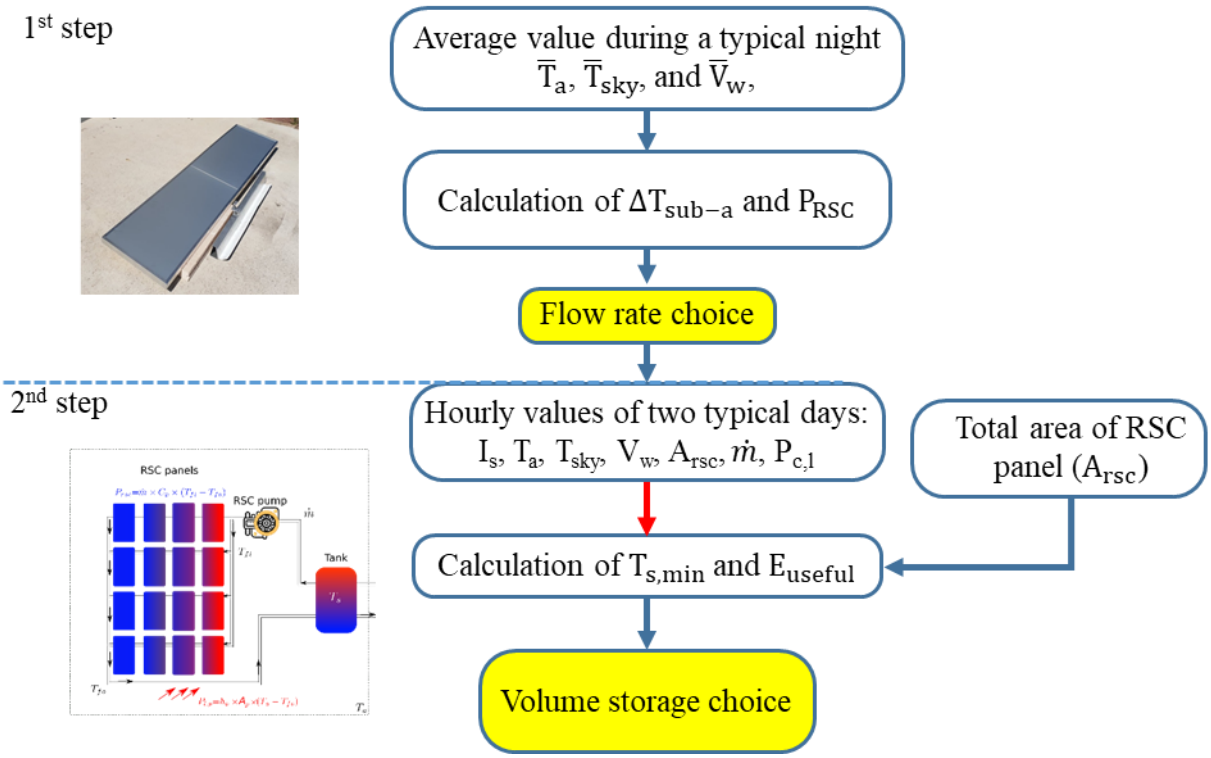


**Figure 3 Sizing method of Radiative Sky Cooling (RSC) system with storage. $A_{RSC}$ is the area of RSC panels (m$^2$). $I_s$ is the short wavelength solar radiation (W m$^{-2}$). $V_s$ is the storage volume for a given area of RSC panels.**

# 4 Application to BaityKool house

In this section, the BaityKool prototype is considered as a case study of the application of the proposed method. This prototype has been developed by the University of Bordeaux, and involves a consortium of 3 Universities (University of Bordeaux in France, An-Najah National University in Nablus-Palestine, Amity University in Dubai-United Arab Emirates), 2 French "*Grandes Écoles*" (*École Nationale Supérieure d'Architecture et de Paysage de Bordeaux*, *École Nationale Supérieure d'Arts et Métiers de Bordeaux*), and an applied research center (Nobatek/INEF4). The BaityKool house has a useful floor area of 80 $m^2$ and was designed with the hot Middle Eastern climate in mind. It uses passive strategies, including a multi-functional innovative exterior wall and a semi-indoor courtyard space. It is powered by Building-Integrated PhotoVoltaic panels (BIPV in an openable-closable canopy over the courtyard to benefit from direct sky radiation during the night, and in the house's East-South-West high-performance concrete skin) and is based on an energy management strategy that aims to reduce consumption while ensuring comfort inside the house (ranked 1$^{st}$ in the Energy Efficiency contest). During the experimental phase of the SDME-2018 competition, a positive energy balance between PV production and consumption for all uses (including an electric vehicle) led to the lowest level of electrical power taken from the grid of all prototypes in competition and a very good level of comfort, controlled regarding temperature, humidity, $CO_2$ and lighting. BaityKool also promotes the use of biological technology in buildings (lumbri-filtration & solar UV grey water treatment, an aquaponic system wall in the courtyard space, and a green roof).

As part of the energy efficiency strategy, an RSC system was designed and installed in the BaityKool house to provide some of its cooling needs.

RSC panels were designed for installation on the roof in order to cool one of the rooms (Kitchen). The architecture of the house is U-shaped, facing north; this means that 3 roof sections are available for the installation of system components (in the East, West and South). The south side is reserved for the solar thermal collectors that produce domestic hot water for the house; thus, two sides (East and West) are available for the installation of the RSC panels (see Figure 4). Considering the dimensions of the panel (600 mm × 1200 mm), and the surface area available on both sides of the roof, 16 RSC panels were installed, with a total surface area of $A_{RSC}$ = 11.5 m².

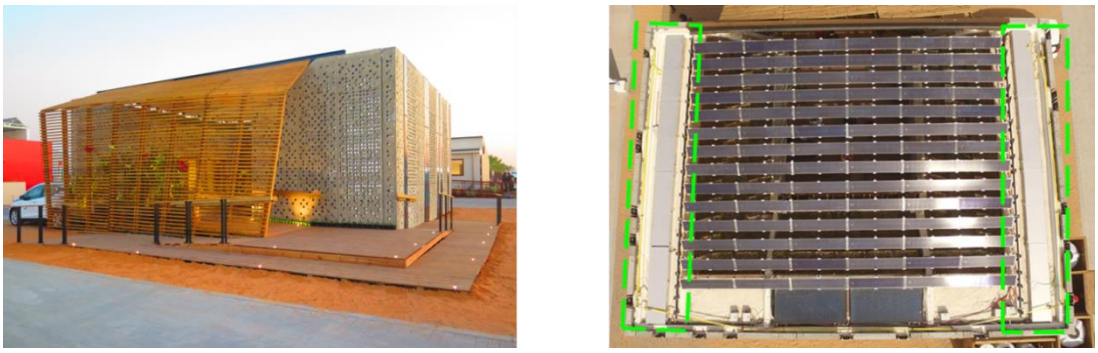

(a) (b)

**Figure 4 (a) BaityKool house during the Solar Decathlon Middle East 2018 in Dubai. (b) Representation of the installation of RSC panels on the roof of the BaityKool house.**

## 4.1 Mass flow rate choice and arrangement of RSC panels

Following the method described in section 3, Figure 5 shows the sub-ambient temperature drop and the cooling power density of the RSC panels for different flow rates in a typical night in Dubai (14-15 November). The calculations are based on the average value of $T_a$, $T_{sky}$ and $V_w$ from 19:00 to 07:00. Remember that here, the RSC system does not operate during the day due to the potentially high solar absorptivity of the anodized surface: cooling needs in the BaityKool prototype that cannot be covered by night free cooling (in Dubai) mostly occur during the summer season (June to September), and during this very hot period, the daytime average effective sky temperature is higher than a reasonable indoor air set-point

temperature (around 26°C, as assumed in this paper). It can be seen in Figure 5 that, at low flow rate values, the temperature difference is maximal (ΔT=4.4°C). In contrast, at high flow rate (4.85 L $min^{-1}$ $m^{-2}$), we obtain the maximum cooling power (50.6 W $m^{-2}$). Depending on the application, the flow rate can be chosen to maximize either the temperature difference ΔT or the cooling power.

In our case, the flow rate is chosen in order to ensure a compromise between cooling power and temperature difference. We chose a flow rate of 0.25 L $min^{-1}$ $m^{-2}$, which corresponds to a sub-ambient temperature $\Delta T_{sub\text{-}a}$=2.1°C and a cooling power density $P_{RSC}/A_{RSC}$ =36.6 W $m^{-2}$. For the total surface area of the panels (11.5 $m^2$), the corresponding value of total mass flow rate that the pump must provide is 172.5 L $h^{-1}$.

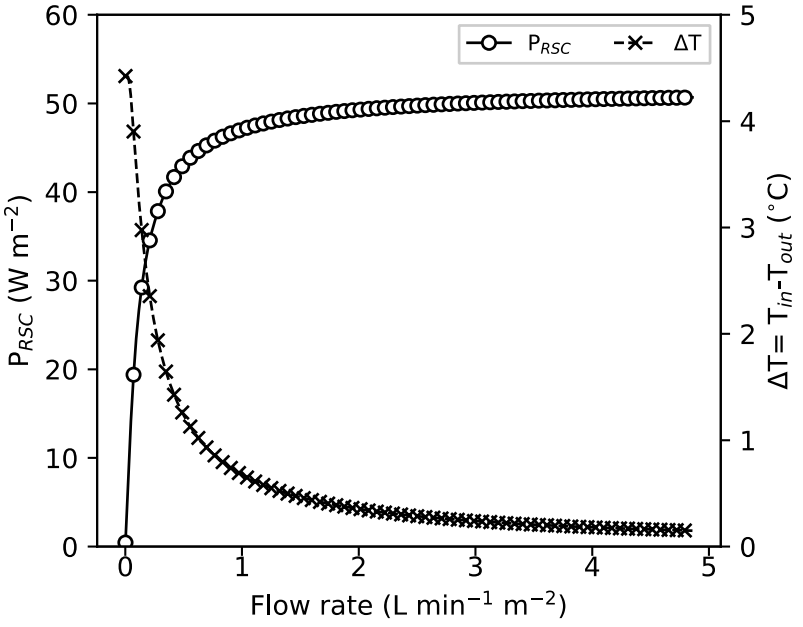


**Figure 5 Cooling power ($P_{RSC}$) (W $m^{-2}$) (black continuous line with round markers) (left y-axis) and sub-ambient temperature drop $\Delta T_{sub\text{-}a}$ (°C) of the Radiative Sky Cooling (RSC) panels (black dashed line with cross markers) (right y-axis) in Dubai during a typical night (14 -15 November).**

BATISOL® panels were designed to support a maximum pressure of 2 bars. Thus, the arrangement of the 16 panels (in series and in parallel) is considered, in order to limit the pressure drop across them to less than 2 bars while minimizing the whole water circuit

284 complexity (for installation and maintenance reasons). Basically, four arrangements are
285 considered:

286 - 1 circuit with 16 panels in series
287 - 2 circuits with 8 panels in series in each circuit
288 - 4 circuits with 4 panels in series in each circuit
289 - 8 circuits with 2 panels in series in each circuit

290 For a total flow rate of 172.5 L $h^{-1}$, the pressure drop values for these four arrangements
291 are presented in Table 1. It considers pressure losses in the circuit panels, regular pressure
292 losses all along the pipes and singular pressure losses due to the different hydraulic
293 accessories used in the installation (elbow, non-return valve, etc.).

294 **Table 1 Pressure drop as a function of number of circuits in the Radiative Sky Cooling (RSC) system**

| Number of circuits | 1 | 2 | 4 | 8 |
|---|---|---|---|---|
| Pressure drop (bar) | 4.8 | 1.88 | 0.93 | 0.46 |

295 It is clear that the three configurations of 2, 4 and 8 circuits allow total pressure on the circuit
296 to be less than 2 bars for a flow rate of 172.5 L $h^{-1}$. We ultimately chose the arrangement of 4
297 circuits with 4 RSC panels in series.

298 ## 4.2 Volume storage choice

299 In order to choose the volume of the storage tank, a simulation was carried out in Dubai
300 climatic conditions during two typical days in winter (from 13 to 15 November). Figure 6
301 shows the solar radiation, wind velocity, effective sky temperature and ambient temperature
302 used as input for the numerical model of the RSC system with storage (effective sky
303 temperature classically referring to an equivalent temperature based on a blackbody radiation
304 hypothesis for the canopy). In the absence of solar radiation, the wind favors convective

contributions that are not beneficial to nocturnal cold production, especially when the temperature of the panels is below ambient temperature ($T_{al}<T_a$, convective heating [12]). On the other hand, the wind is beneficial when the panel temperature is higher than the ambient temperature ($T_{al}>T_a$, convective cooling [44]).

Furthermore, a daily cooling load profile was used to represent the cooling load in one of the BaityKool rooms (Room-kitchen-area=10.5 m²). During this period, external ambient air temperature ranges from 22.7°C to 31.4°C. In addition, the effective sky temperature varies between 9.9°C and 15.4°C. Solar irradiance peaked at 616.1 W $m^{-2}$ on November 13. The cooling load represented in Figure 7 was estimated considering thermal gains through the walls, solar gains through the window, and thermal gains of the occupants in the room for a typical day in Dubai during the winter. The energy required to maintain the room temperature at 26°C is 1.4 kWh $day^{-1}$. In this section on sizing, the pipes of the RSC system are assumed to be well insulated so that heat losses (gains) are negligible.

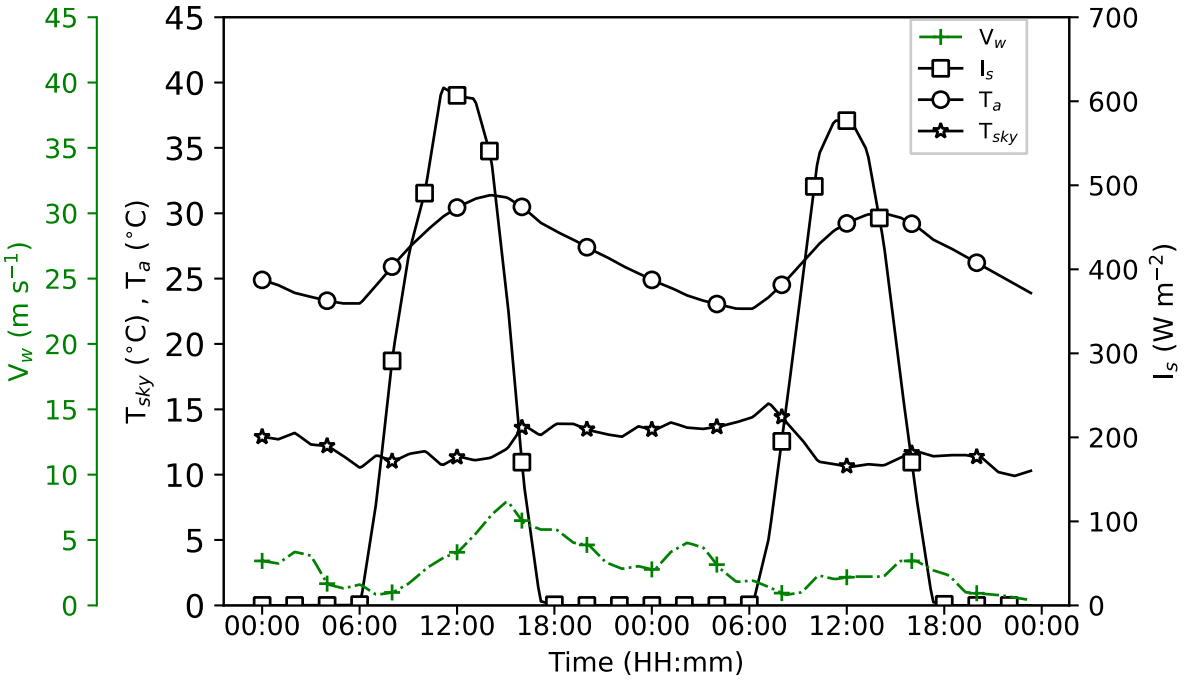


**Figure 6 Meteorological conditions on 13 and 14 November in Dubai: black line with round markers represents ambient air temperature ($T_a$) (°C). Black continuous line with star markers represents effective sky temperature ($T_{sky}$)**

**(°C). Green dash-dotted line with cross markers represents wind velocity ($V_w$) (m $s^{-1}$). Black line with square markers represents solar irradiance ($I_s$) (W $m^{-2}$).**

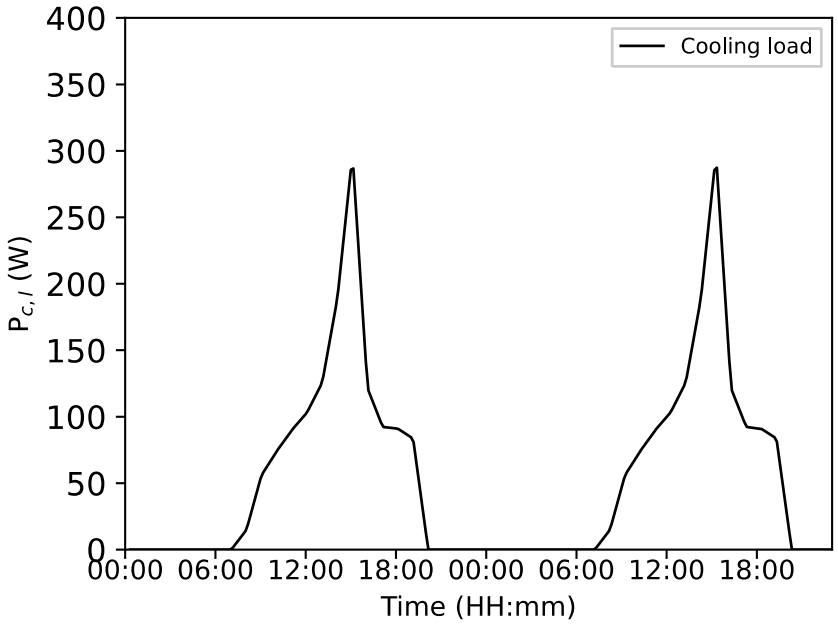


**Figure 7 Cooling load ($P_{c,l}$) (W) of the room in BaityKool between 13 and 14 November in Dubai.**

Figure 8 shows the water storage temperature for different values of the water volume tank. Regardless of the storage volume, the RSC cold production contributes to the decrease in the water storage temperature during the night to below the ambient temperature, due to the radiative heat exchange of the RSC panels with the sky (canopy). This water storage temperature follows the variation in the cooling load with a phase shift and damping that depends on the storage volume. By increasing the storage volume from 100 L to 1000 L, the maximum value of the water storage temperature decreases from 29.1 to 24.8°C while the phase shift increases from 1 hour and 20 minutes to 5 hours and 20 minutes, and the minimum water storage temperature increases from 19.7 to 22.8°C.

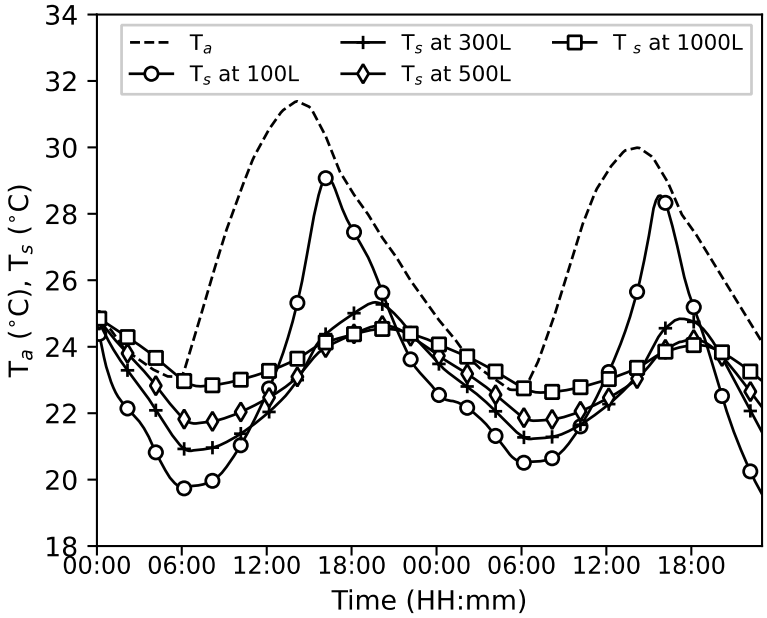


**Figure 8 Ambient air temperature ($T_a$) (°C) (black dashed line) and water storage temperature ($T_s$) (°C) for different storage volumes: 100 L (black continuous line with round markers), 300 L (black continuous line with cross markers), 500 L (black continuous line with diamond markers) and 1000 L (black continuous line with square markers), between 13 and 14 November in Dubai.**

Figure 9 represents both the *minimum* value of the water storage temperature and the useful energy stored in the tank, versus the storage volume. As mentioned before, this minimal value increases by about 3.3°C (19.3 to 22.6°C) as the tank volume increases from 100 L to 1000 L, and remains below the desired value for the internal air temperature (26°C). In terms of useful energy, Figure 9 shows that it increases (from 0.7 kWh to 3.9 kWh) with the storage volume. Note also that the storage volume that corresponds to the energy needed for cooling the room (1.4 kWh) is 217 L. To ensure this cooling load during the SMDE 2018 competition we chose to oversize this storage and installed a 300-liter storage tank in the BaityKool house.

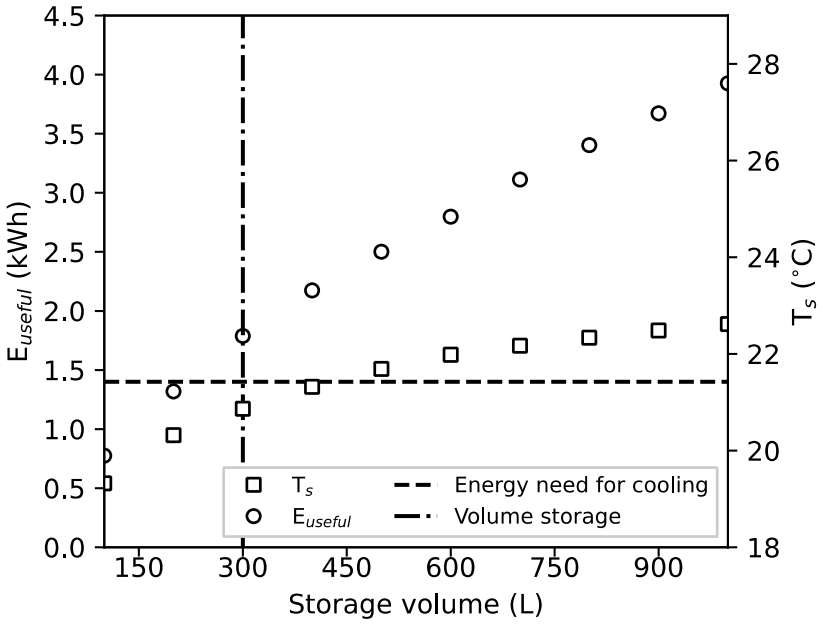


348

349 **Figure 9 Minimal storage temperature ($T_s$) (°C) (black square markers) and useful energy stored ($E_{usefull}$) (kWh)**
350 **(black round markers) versus storage volume. Horizontal black dashed line represents the energy needed to cool the**
351 **room (1.4 kWh) corresponding to the storage volume (300 L) (vertical black dash-dotted line).**

352 # 5 Experimental platform and instrumentation

353 Sixteen RSC panels are installed on the roof of BaityKool, arranged in 4 circuits in
354 parallel (4 panels in series in each circuit) with a total area of 11.5 m². The pipes are insulated
355 with 19 mm of black rubber insulation pipe. The outlet water temperature of the RSC panels
356 is measured using a PT100 temperature sensor (Produal TEP NTC 100, ±0.5°C accuracy).
357 This is installed on one circuit and mounted on the pipe by means of an adjustable tie. For the
358 storage tank, a commercial Solerio H300 from Atlantic is used (Volume of water 300 L,
359 $U \cdot A$=2.75 W $K^{-1}$). The storage temperature is measured using a PT100 (TEY4 NTC 10,
360 ±0.5°C accuracy) placed half-way up the water tank in a position specified by the
361 manufacturer. Total flow rate is measured by an ultrasonic flow sensor (Belimo FM015R-SZ,
362 ±6% accuracy). Temperature and flow rate data are monitored and stored using a building
363 automation system from Distech Controls.

The effective sky temperature ($T_{sky}$) is measured using a pyrgeometer SGR3-V (Kipp & Zonen, <5% accuracy). Data are stored on the computer using Smart Explorer software from Kipp & Zonen. For the weather conditions, a weather station (Vintage pro2 plus from Davis instruments) is installed on the roof of BaityKool. It measures and stores data for ambient temperature (±0.5 K accuracy), air relative humidity (±2% accuracy), solar irradiance (±5% accuracy), wind direction (±3° accuracy) and wind velocity (±3 km $h^{-1}$ accuracy).

# 6 Experimental evaluation of the energy performance in Dubai

In order to evaluate the thermal performance of the installed RSC system with storage, we carried out an experimental test consisting of three successive nights' cooling without daily cold diffusion (only cold production by RSC panels and cold storage in the tank).

Figure 10 shows the weather conditions during the test phase from 2 to 5 December 2019. The ambient temperature varies between 29°C during daytime and 14°C during night-time. The maximal effective sky temperature is reached during the first day with a value of $T_{sky}$=21°C while the minimal temperature is reached during the second night with a value of $T_{sky}$=2.5°C. During this period, solar irradiance reaches its maximum value (800 W $m^{-2}$) on December 5.

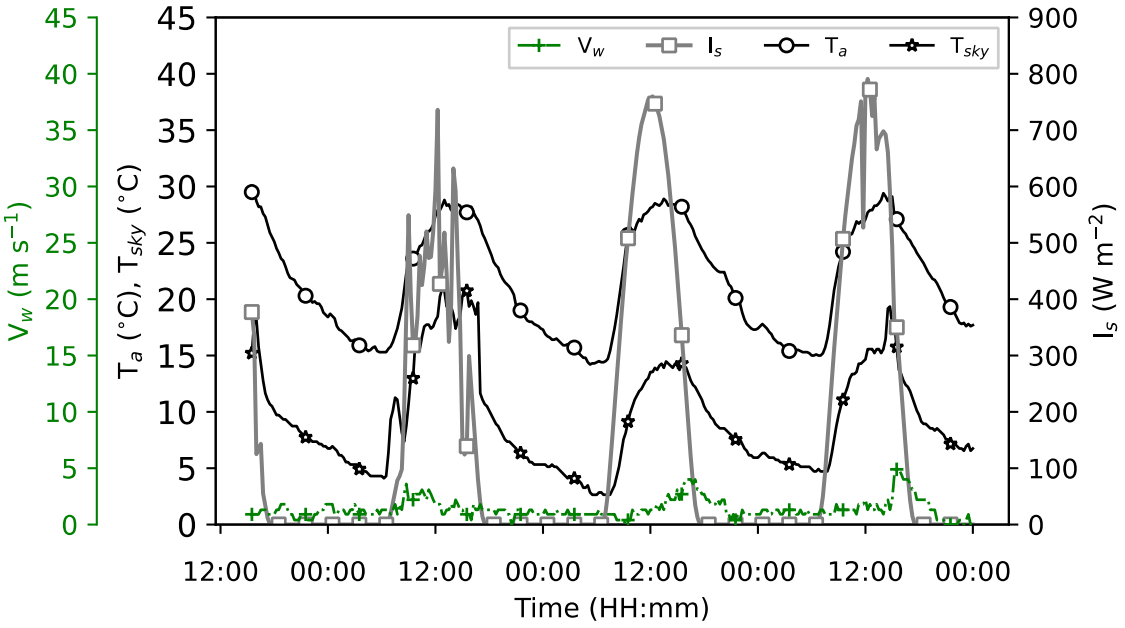


**Figure 10 Weather conditions in Dubai from 2 to 5 December 2019. Black solid line with round markers represents ambient air temperature ($T_a$) (°C). Black solid line with star markers represents effective sky temperature ($T_{sky}$) (°C). Green dash-dotted line with cross markers represents wind velocity ($V_w$) (m s$^{-1}$). Grey line with square markers represents solar irradiance ($I_s$) (W m$^{-2}$).**

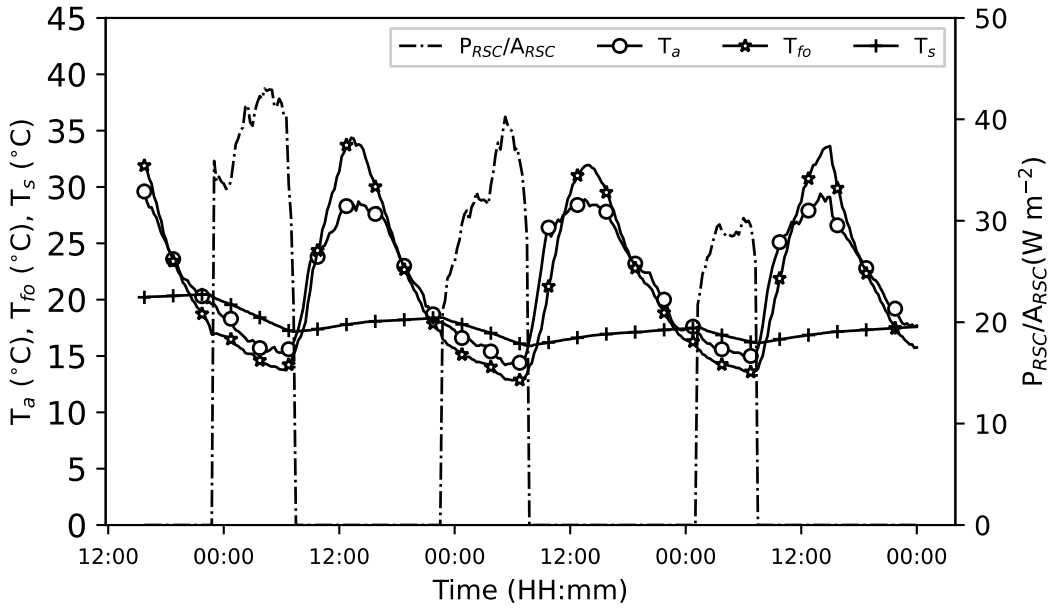


**Figure 11 Radiative Sky Cooling (RSC) panels outlet temperature ($T_{fo}$) (°C) (black dash-dotted line with star markers), storage tank temperature ($T_s$) (°C) (black continuous line with cross markers), ambient air temperature ($T_a$) (°C) (black continuous line with round markers), and cooling power density ($P_{RSC}/A_{RSC}$) (W m$^{-2}$) (black solid line with star markers) (right y-axis) (when the pump between the panels and the storage tank is in operation). From 2 to 5 December 2019 in Dubai.**

Figure 11 illustrates the thermal performance of the RSC system in terms of temperature and cooling power density from 2 to 5 December 2019. The water mass flow rate is 110 L $h^{-1}$, which is less than the sized value. This is mainly due to the choice of pump and the excessive pressure drop in the RSC system hydraulic circuit (a consequence of some unexpected pipe elbows which were added to the BaityKool hydraulic circuit during assembly). Due to the radiative Sky Cooling phenomenon, the outlet water temperature of the RSC panels is below the ambient temperature during the three successive nights by a maximum of $\Delta T_{sub\text{-}a}$ = 2.8°C. Average cooling power density is between 30 W $m^{-2}$ and 45 W $m^{-2}$. This cold production resulted in a decrease in the storage tank temperature from 20.2°C to 17.7°C during the first night, from 18.4°C to 15.9°C during the second night, and from 17.6°C to 16.0°C during the third night. We notice a slight increase in the storage temperature during the day because of heat losses from the tank into the ambient air.

In order to identify the average heat loss coefficient in the pipe and hydraulic accessories $h_p$, the model of the RSC system proposed in section 2.2 is considered, together with the weather conditions from 2 to 6 December and the monitored flow rate value. The following Root Mean Square Error (RMSE) is then computed (Eq. 11):

$$RMSE = \sqrt{\frac{1}{n}\sum_{i=1}^{n}(T_{s,num,i} - T_{s,exp,i})^2} \qquad \text{Eq. 11}$$

where $T_{s,num,i}$ and $T_{s,exp,i}$ are the modeled and measured water storage temperature (K) respectively.

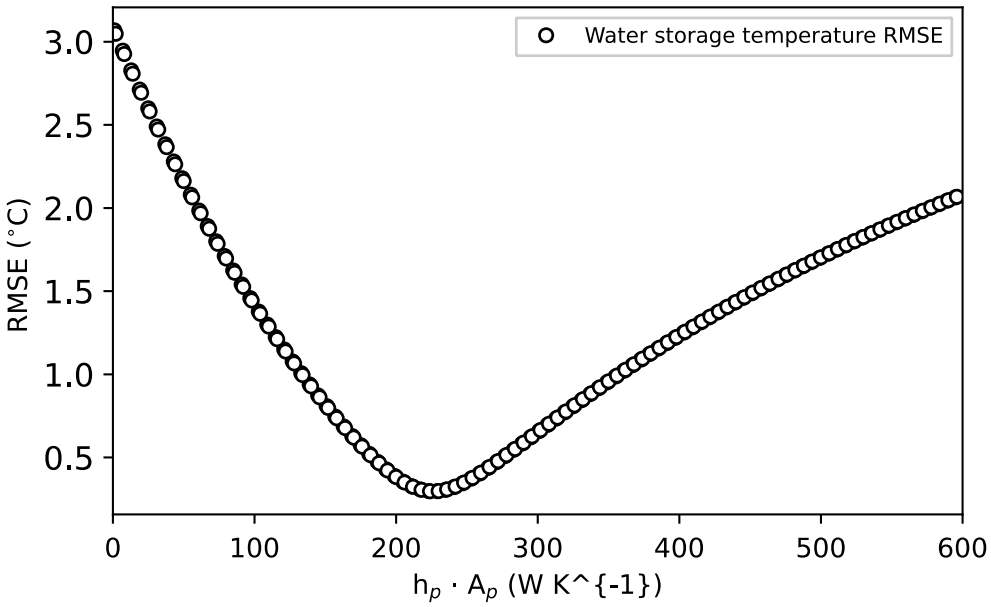


409

410 **Figure 12 Identification of heat loss in the hydraulic circuit of the RSC system: water storage temperature RSME (°C)**
411 **versus water-pipe heat exchange coefficient considering area of the pipe $h_p \cdot A_p$ (W K$^{-1}$).**

412 Figure 12 shows a *minimum* value of RMSE (0.29°C) for a value of the heat exchange
413 coefficient $h_p \cdot A_p$=226 W K$^{-1}$. Corresponding numerical values in terms of water storage
414 temperature $T_s$ and RSC outlet temperature $T_{fo}$ are compared to experimental values in Figures
415 13(a) and 13(b) respectively, confirming good agreement between experimental and
416 simulation results for this $h_p$ value. In Figures 13(a) and 13(b), simulation results for $h_p \cdot A_P$ = 0
417 W K$^{-1}$ are also proposed for $T_s$, $P_{RSC}/A_{RSC}$ and $T_{fo}$, in order to estimate the impact of insulating
418 pipes and hydraulic accessories on the RSC system performances: better insulation of the
419 pipes and hydraulic accessories will certainly reduce the heat gains and the stored water
420 storage temperature considerably.

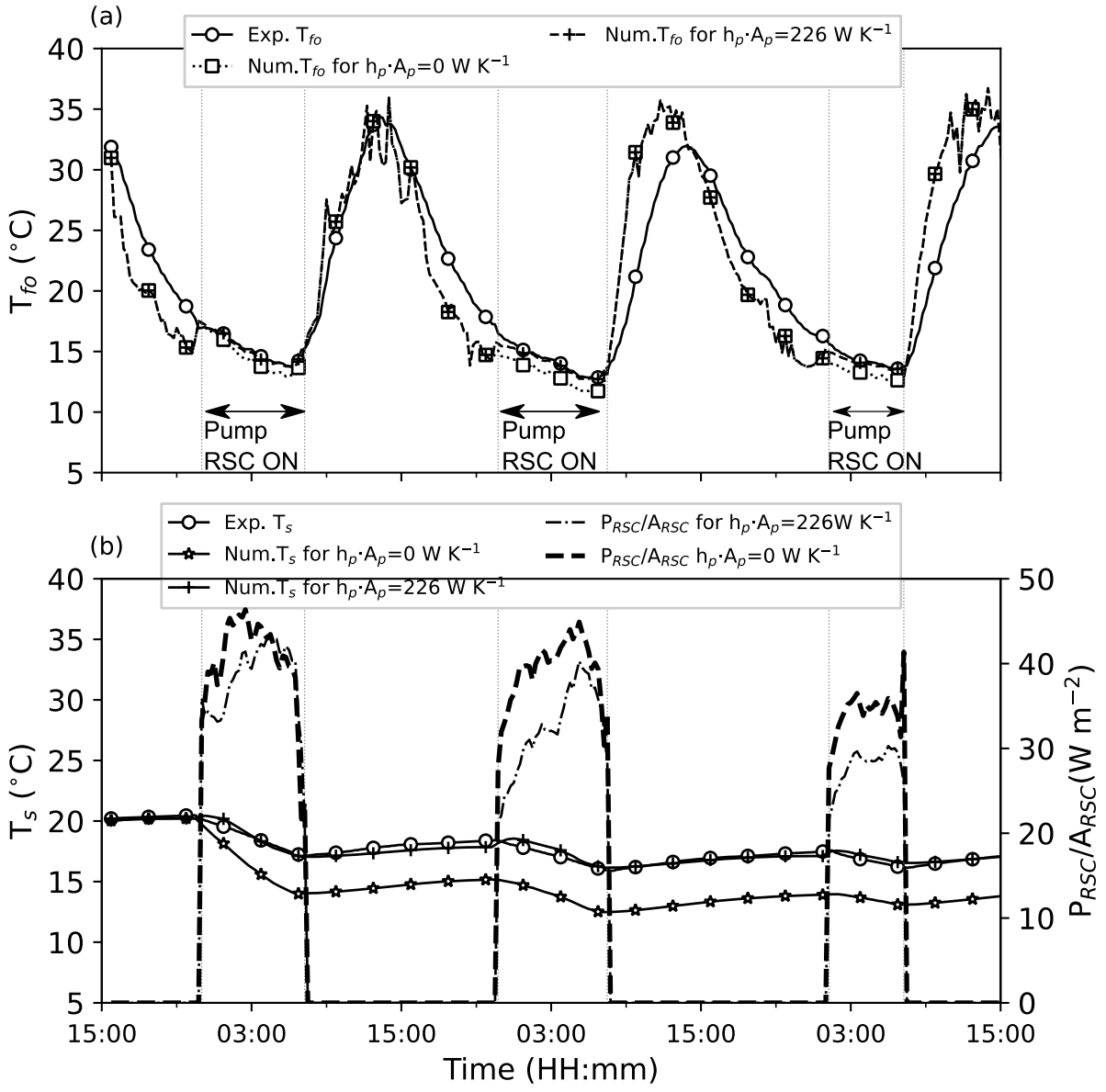


**Figure 13 (a) Experimental results of Radiative Sky Cooling (RSC) outlet temperature ($T_{fo}$) (black continuous line with round markers) and numerical results of RSC $T_{fo}$ for $h_p \cdot A_p$ = 0 W K$^{-1}$ (black dotted line with square markers) and $h_p \cdot A_p$ = 226 W K$^{-1}$ (black dashed line with cross markers). (b) Experimental results and water Storage temperature ($T_s$) (°C) (black continuous line with round markers), numerical results of $T_s$ for $h_p \cdot A_p$ = 0 W K$^{-1}$ (black continuous line with star markers) and $h_p \cdot A_p$ = 226 W K$^{-1}$ (black continuous line with cross markers), cooling power density ($P_{RSC}/A_{RSC}$) (W m$^{-2}$) for $h_p A_p$ = 226 W/K (tiny black dash-dotted line) and for $h_p \cdot A_p$ = 0 W K$^{-1}$ (large black dashed line) (right y-axis).**

Considering periods of pump operation in the case of $h_p \cdot A_p$ = 0 W K$^{-1}$, Figure 13b shows that the storage temperature varies on average between 17.1±0.3°C and 18.8±1.2°C while the effective sky temperature in Dubai varies from 4.1±1.1 to 5.8±1.1°C (see Figure

10). The corresponding $P_{RSC}/A_{RSC}$ produced during pump activation is about 37.9±2.5 W m$^{-2}$ (see Figure 13b). The temperature difference between the indoor set-point temperature (26°C in our case) and the sky ranges from approximately 20.2 and 21.9°C. This temperature difference provides important information for estimating the ability and the performance of the RSC system with cold storage to meet the cooling needs in a given place-location and time-period relying solely on knowledge of the average effective night-time sky temperature. With an appropriate indoor set-point temperature, knowing the average effective night-time sky temperature will allow rapid assessment of the cooling potential of such a system. According to our results, a temperature difference of 20°C indicates a significant potential (slightly less than 40 W m$^{-2}$) that could be exploited for such a water RSC cooling production and storage system.

# 7 Conclusion

In the present study, we propose a sizing method for a night-time radiative sky cooling system that includes water storage, mostly for day-time cooling uses, based on four performance indicators (sub-ambient temperature, cooling power density, *minimum* storage temperature and useful stored energy). Using these indicators, it is possible to choose the operational water flow rate in cooling generation (for a fixed value of the area intended for the radiative sky cooling panels) and in the storage volume, in order to cover cooling needs. This method was applied to the BaityKool project, a house prototype built in the Dubai desert (United Arab Emirates, UAE) for the Solar Decathlon Middle East 2018 competition. A case study was conducted on part of the BaityKool prototype, a living zone with an area of 10.5 m². Using a 0.3 m$^3$ cold storage tank and a radiative sky cooling area of 11.5 m$^2$, the experimental campaign was carried out over 3 successive nights and noted an average cooling production of between 30 and 45 W m$^{-2}$. These results indicate that the insulation of the

hydraulic circuits is of crucial importance and has a considerable influence on the system performance in terms of production and storage.

It is expected that the proposed sizing method can be used as a design support tool for engineers and researchers to design successful and economically competitive radiative sky cooling systems under other weather conditions (e.g. northern Mediterranean or near-oceanic climates). An initial assessment should be based on the temperature difference ($\Delta T$) between the desired indoor set-point temperature and the mean effective night-time sky temperature in the considered location. Once the cooling potential is proven ($\Delta T$>20°C), the method proposed in this article can be applied to size the elements that make up the radiative sky cooling system with storage consistent with part or all of the building's the cooling needs and architectural considerations such as available roof area.

In order to improve the overall performance of the system, future work could assess systems integrating both the production of cold by radiative sky cooling (overnight) and a heat supply or domestic hot water production using solar energy (during the daytime), through the same panels. The hydraulic operations of the two production modes are very similar, although the production potential (power densities) differs significantly for these two renewable energy resources.

## Acknowledgments

This research was funded by the *Région Nouvelle-Aquitaine* under CRA LABCOM INEF4 2019 grant number 3798420-3796420. We would like to thank the technicians and engineers of the BaityKool living lab project for their help in the implementation of the study site, the acquisition system and the data.

# References


[1] M.M. Rahman, M.G. Rasul, M.M.K. Khan, Energy conservation measures in an institutional building in sub-tropical climate in Australia, Applied Energy. 87 (2010) 2994–3004. https://doi.org/10.1016/j.apenergy.2010.04.005.

[2] M.I. Ahmad, H. Jarimi, S. Riffat, Potentials of Nocturnal Cooling in Various Locations/Countries and Climatic Conditions, in: Nocturnal Cooling Technology for Building Applications, Springer Singapore, Singapore, 2019: pp. 51–61. https://doi.org/10.1007/978-981-13-5835-7_5.

[3] H. Chen, Z. Li, B. Sun, Performance evaluation and parametric analysis of an integrated diurnal and nocturnal cooling system driven by photovoltaic-thermal collectors with switchable film insulation, Energy Conversion and Management. 254 (2022) 115197. https://doi.org/10.1016/j.enconman.2021.115197.

[4] M. Farmahini Farahani, G. Heidarinejad, S. Delfani, A two-stage system of nocturnal radiative and indirect evaporative cooling for conditions in Tehran, Energy and Buildings. 42 (2010) 2131–2138. https://doi.org/10.1016/j.enbuild.2010.07.003.

[5] D. Zhao, A. Aili, X. Yin, G. Tan, R. Yang, Roof-integrated radiative air-cooling system to achieve cooler attic for building energy saving, Energy and Buildings. 203 (2019) 109453. https://doi.org/10.1016/j.enbuild.2019.109453.

[6] G.N. Nwaji, C.A. Okoronkwo, N. V. Ogueke, E.E. Anyanwu, Hybrid solar water heating/nocturnal radiation cooling system I: A review of the progress, prospects and challenges, Energy and Buildings. 198 (2019) 412–430. https://doi.org/10.1016/j.enbuild.2019.06.017.

[7] Z. Liu, H. Tan, G. Ma, Experimental investigation on night sky radiant cooling performance of duct-type heat exchanger, International Journal of Ventilation. 16 (2017) 255–267. https://doi.org/10.1080/14733315.2017.1299520.

[8] F. Rubel, K. Brugger, K. Haslinger, I. Auer, The climate of the European Alps: Shift of very high resolution Köppen-Geiger climate zones 1800–2100, Meteorologische Zeitschrift. (2017) 115–125. https://doi.org/10.1127/metz/2016/0816.

[9] M.G. Meir, J.B. Rekstad, O.M. LØvvik, A study of a polymer-based radiative cooling system, Solar Energy. 73 (2002) 403–417. https://doi.org/10.1016/S0038-092X(03)00019-7.

[10] M.A. Al-Nimr, Z. Kodah, B. Nassar, A theoretical and experimental investigation of a radiative cooling system, Solar Energy. 63 (1998) 367–373. https://doi.org/10.1016/S0038-092X(98)00098-X.

[11] A. Dimoudi, A. Androutsopoulos, The cooling performance of a radiator based roof component, Solar Energy. 80 (2006) 1039–1047. https://doi.org/10.1016/j.solener.2005.06.017.

[12] J.A.F. Tevar, S. Castaño, A.G. Marijuán, M.R. Heras, J. Pistono, Modelling and experimental analysis of three radioconvective panels for night cooling, Energy and Buildings. 107 (2015) 37–48. https://doi.org/10.1016/j.enbuild.2015.07.027.

[13] C.A. Okoronkwo, K.N. Nwigwe, N. V Ogueke, E.E. Anyanwu, D.C. Onyejekwe, P.E. Ugwuoke, An Experimental Investigation of the Passive Cooling of a Building Using Nighttime Radiant Cooling, International Journal of Green Energy. 11 (2014) 1072–1083. https://doi.org/10.1080/15435075.2013.829775.

[14] B. Bokor, H. Akhan, D. Eryener, M. Horváth, Nocturnal passive cooling by transpired solar collectors, Applied Thermal Engineering. 188 (2021) 116650. https://doi.org/10.1016/j.applthermaleng.2021.116650.

[15] U. Eicker, A. Dalibard, Photovoltaic-thermal collectors for night radiative cooling of buildings, Solar Energy. 85 (2011) 1322–1335. https://doi.org/10.1016/j.solener.2011.03.015.

[16] B. Zhao, M. Hu, X. Ao, G. Pei, Conceptual development of a building-integrated photovoltaic–radiative cooling system and preliminary performance analysis in Eastern China, Applied Energy. 205 (2017) 626–634. https://doi.org/10.1016/j.apenergy.2017.08.011.

[17] T.H. Kwan, D. Gao, B. Zhao, X. Ren, T. Hu, Y.N. Dabwan, G. Pei, Integration of radiative sky cooling to the photovoltaic and thermoelectric system for improved space cooling, Applied Thermal Engineering. 196 (2021) 117230. https://doi.org/10.1016/j.applthermaleng.2021.117230.

[18] Z. Aketouane, M. Malha, D. Bruneau, P. Lagiere, S. Raji, P. Bonnamy, B. Durand-Estebe, A. Bah, Couplage d'une PAC et d'un système de refroidissement d'eau par échanges radiatifs avec le ciel : modélisation et estimation de performances, in: International Building Performance Simulation Association (IBPSA) France, hal, Bordeaux, 2018.

[19] H. Bao, C. Yan, B. Wang, X. Fang, C.Y. Zhao, X. Ruan, Double-layer nanoparticle-based coatings for efficient terrestrial radiative cooling, Solar Energy Materials and Solar Cells. 168 (2017) 78–84. https://doi.org/10.1016/j.solmat.2017.04.020.

[20] L. Evangelisti, C. Guattari, F. Asdrubali, On the sky temperature models and their influence on buildings energy performance: A critical review, Energy and Buildings. 183 (2019) 607–625. https://doi.org/10.1016/j.enbuild.2018.11.037.

[21] A.S. Farooq, P. Zhang, Y. Gao, R. Gulfam, Emerging radiative materials and prospective applications of radiative sky cooling - A review, Renewable and Sustainable Energy Reviews. 144 (2021) 110910. https://doi.org/10.1016/j.rser.2021.110910.

[22] A.R. Gentle, G.B. Smith, Radiative heat pumping from the Earth using surface phonon resonant nanoparticles, Nano Letters. 10 (2010) 373–379. https://doi.org/10.1021/nl903271d.

553 [23] M. Hu, G. Pei, L. Li, R. Zheng, J. Li, J. Ji, Theoretical and Experimental Study of
554 Spectral Selectivity Surface for Both Solar Heating and Radiative Cooling, 2015 (2015).
555 [24] J. Kou, Z. Jurado, Z. Chen, S. Fan, A.J. Minnich, Daytime Radiative Cooling Using
556 Near-Black Infrared Emitters, ACS Photonics. 4 (2017) 626–630.
557 https://doi.org/10.1021/acsphotonics.6b00991.
558 [25] A.P. Raman, M.A. Anoma, L. Zhu, E. Rephaeli, S. Fan, Passive radiative cooling below
559 ambient air temperature under direct sunlight, Nature. 515 (2014) 540–544.
560 https://doi.org/10.1038/nature13883.
561 [26] E. Rephaeli, A. Raman, S. Fan, Ultrabroadband Photonic Structures To Achieve High-
562 Performance Daytime Radiative Cooling, Nano Lett. 13 (2013) 1457–1461.
563 https://doi.org/10.1021/nl4004283.
564 [27] C.N. Suryawanshi, C.T. Lin, Radiative cooling: Lattice quantization and surface
565 emissivity in thin coatings, ACS Applied Materials and Interfaces. 1 (2009) 1334–1338.
566 https://doi.org/10.1021/am900200r.
567 [28] Zhai Yao, Ma Yaoguang, David Sabrina N., Zhao Dongliang, Lou Runnan, Tan Gang,
568 Yang Ronggui, Yin Xiaobo, Scalable-manufactured randomized glass-polymer hybrid
569 metamaterial for daytime radiative cooling, Science. 355 (2017) 1062–1066.
570 https://doi.org/10.1126/science.aai7899.
571 [29] E.A. Goldstein, A.P. Raman, S. Fan, Sub-ambient non-evaporative fluid cooling
572 with the sky, Nature Energy. 2 (2017) 17143. https://doi.org/10.1038/nenergy.2017.143.
573 [30] A.R. Gentle, G.B. Smith, A Subambient Open Roof Surface under the Mid-Summer
574 Sun, Adv. Sci. 2 (2015) 1500119. https://doi.org/10.1002/advs.201500119.
575 [31] D. Zhao, A. Aili, Y. Zhai, J. Lu, D. Kidd, G. Tan, X. Yin, R. Yang, Subambient Cooling
576 of Water: Toward Real-World Applications of Daytime Radiative Cooling, Joule. 3
577 (2019) 111–123. https://doi.org/10.1016/j.joule.2018.10.006.

[32] G. Heidarinejad, M. Farmahini Farahani, S. Delfani, Investigation of a hybrid system of nocturnal radiative cooling and direct evaporative cooling, Building and Environment. 45 (2010) 1521–1528. https://doi.org/10.1016/j.buildenv.2010.01.003.

[33] Z. Aketouane, M. Malha, D. Bruneau, A. Bah, B. Michel, M. Asbik, O. Ansari, Energy savings potential by integrating Phase Change Material into hollow bricks: The case of Moroccan buildings, Building Simulation. 11 (2018) 1109–1122. https://doi.org/10.1007/s12273-018-0457-5.

[34] N. Fernandez, W. Wang, K. Alvine, K. S, Energy Savings Potential of Radiative Cooling Technologies, (2015) 72.

[35] J. Liu, J. Yuan, J. Zhang, H. Tang, K. Huang, J. Xing, D. Zhang, Z. Zhou, J. Zuo, Performance evaluation of various strategies to improve sub-ambient radiative sky cooling, Renewable Energy. 169 (2021) 1305–1316. https://doi.org/10.1016/j.renene.2021.01.103.

[36] A. Aili, D. Zhao, J. Lu, Y. Zhai, X. Yin, G. Tan, R. Yang, A kW-scale, 24-hour continuously operational, radiative sky cooling system: Experimental demonstration and predictive modeling, Energy Conversion and Management. 186 (2019) 586–596. https://doi.org/10.1016/j.enconman.2019.03.006.

[37] Solar Decathlon Middle East Dubai, (2018). https://www.solardecathlonme.com/ (accessed November 2, 2021).

[38] A.K. Samuel, V. Mohanan, A. Sempey, F.Y. Garcia, P. LAGIERE, D. Bruneau, N. Mahanta, A Sustainable Approach for a Climate Responsive House in UAE: Case Study of SDME 2018 BAITYKOOL Project, in: 2019 International Conference on Computational Intelligence and Knowledge Economy (ICCIKE), 2019: pp. 816–823. https://doi.org/10.1109/ICCIKE47802.2019.9004235.

602 [39] R.G. Martinez, B.A. Goikolea, I.G. Paya, P. Bonnamy, S. Raji, J. Lopez, Performance
603 assessment of an unglazed solar thermal collector for envelope retrofitting, Energy
604 Procedia. 115 (2017) 361–368. https://doi.org/10.1016/j.egypro.2017.05.033.
605 [40] Themacs engineering, (2018). https://themacs-engineering.com/en/emissivity/ (accessed
606 November 2, 2021).
607 [41] J. a. Duffie, W. a. Beckman, W.M. Worek, Solar Engineering of Thermal Processes, 4nd
608 ed., 2003. https://doi.org/10.1115/1.2930068.
609 [42] M. Zeyghami, D.Y. Goswami, E. Stefanakos, A review of clear sky radiative cooling
610 developments and applications in renewable power systems and passive building
611 cooling, Solar Energy Materials and Solar Cells. 178 (2018) 115–128.
612 https://doi.org/10.1016/j.solmat.2018.01.015.
613 [43] ANSI/ASHRAE 55-2013, Thermal Environmental Conditions for Human Occupancy.
614 Atlanta, USA: American Society of Heating, Refrigerating and Air-Conditioning
615 Engineers., (2013).
616 [44] A. Shitzer, Assessment of the effects of environmental radiation on wind chill equivalent
617 temperatures, Eur J Appl Physiol. 104 (2008) 215–220. https://doi.org/10.1007/s00421-
618 007-0624-3.